Block-Based Adaptive Mesh Refinement scheme based on numerical density of entropy production for conservation laws and applications.

Mehmet Ersoy [1],
Frédéric Golay, Lyudmyla Yushchenko, Université de Toulon, IMATH,
and Damien Sous, Aix-Marseille Université, CNRS/INSU, IRD, MIO

International meeting AMS/EMS/SPM
Partial Differential Equations: Ambitious Mathematics for Real-life Applications

2015, 10-13 June, Porto, Portugal

1. *Mehmet.Ersoy@univ-tln.fr*

- Physical motivations : to be able to simulate applications in real-life fluid mechanics in dimension 2 and 3
  - wave-breaking,
  - wave-impacting,
  - tsunami . . .

- Physical motivations : to be able to simulate applications in real-life fluid mechanics in dimension 2 and 3
    - wave-breaking,
    - wave-impacting,
    - tsunami ...
- Numerical motivations : to be able to design a model and a numerical code for such applications
    - fast and accurate,
    - limiting the numerical diffusion,
    - adaptive and a suitable meshing machinery,
    - optimized numerical code,
    - ...

Motivations

- Physical motivations : to be able to simulate applications in real-life fluid mechanics in dimension 2 and 3
  - wave-breaking,
  - wave-impacting,
  - tsunami . . .
- Numerical motivations : to be able to design a model and a numerical code for such applications
  - fast and accurate,
  - limiting the numerical diffusion,
  - adaptive and a suitable meshing machinery,
  - optimized numerical code,
  - . . .
- Mathematical motivations : introducing new tools
  - a suitable mesh refinement tool and its mathematical properties
  - consistency at interface of two cells of different level,
  - . . .

Outline of the talk

1. Principle of the method
   - Generality
   - 1d examples and local time stepping
   - Data structure : BB-AMR
2. Applications
   - The two phase low Mach model
   - A two-dimensional dam-break problem
   - A three-dimensional dam-break problem
3. Conclusions

OUTLINE

1. PRINCIPLE OF THE METHOD
   - Generality
   - 1d examples and local time stepping
   - Data structure : BB-AMR

2. APPLICATIONS
   - The two phase low Mach model
   - A two-dimensional dam-break problem
   - A three-dimensional dam-break problem

3. CONCLUSIONS

Outline

1. Principle of the method
   - Generality
   - 1d examples and local time stepping
   - Data structure : BB-AMR
2. Applications
   - The two phase low Mach model
   - A two-dimensional dam-break problem
   - A three-dimensional dam-break problem
3. Conclusions

We focus on general non linear hyperbolic conservation laws

$$\left\{ \begin{array}{l} \dfrac{\partial \boldsymbol{w}}{\partial t} + \dfrac{\partial \boldsymbol{f}(\boldsymbol{w})}{\partial x} = 0,\ (t,x) \in \mathbb{R}^+ \times \mathbb{R} \\ \boldsymbol{w}(0,x) = \boldsymbol{w}_0(x),\ x \in \mathbb{R} \end{array} \right.$$

$\boldsymbol{w} \in \mathbb{R}^d$	:	vector state,
$\boldsymbol{f}$	:	flux governing the physical description of the flow.

We focus on general non linear hyperbolic conservation laws

$$\left\{ \begin{array}{l} \dfrac{\partial \boldsymbol{w}}{\partial t} + \dfrac{\partial \boldsymbol{f}(\boldsymbol{w})}{\partial x} = 0, \ (t,x) \in \mathbb{R}^+ \times \mathbb{R} \\ \boldsymbol{w}(0,x) = \boldsymbol{w}_0(x), \ x \in \mathbb{R} \end{array} \right.$$

Weak solutions satisfy

$$S = \frac{\partial s(\boldsymbol{w})}{\partial t} + \frac{\partial \psi(\boldsymbol{w})}{\partial x} \left\{ \begin{array}{lll} = & 0 & \text{for smooth solution} \\ = & 0 & \text{across rarefaction} \\ < & 0 & \text{across shock} \end{array} \right.$$

where (s, ψ) stands for a convex entropy-entropy flux pair :

$$(\nabla \psi(\boldsymbol{w}))^T = (\nabla s(\boldsymbol{w}))^T \ D_{\boldsymbol{w}} \boldsymbol{f}(\boldsymbol{w})$$

We focus on general non linear hyperbolic conservation laws

$$\begin{cases} \dfrac{\partial \boldsymbol{w}}{\partial t} + \dfrac{\partial \boldsymbol{f}(\boldsymbol{w})}{\partial x} = 0, \ (t,x) \in \mathbb{R}^+ \times \mathbb{R} \\ \boldsymbol{w}(0,x) = \boldsymbol{w}_0(x), \ x \in \mathbb{R} \end{cases}$$

Weak solutions satisfy

$$S = \frac{\partial s(\boldsymbol{w})}{\partial t} + \frac{\partial \psi(\boldsymbol{w})}{\partial x} \begin{cases} = & 0 & \text{for smooth solution} \\ = & 0 & \text{across rarefaction} \\ < & 0 & \text{across shock} \end{cases}$$

where (s, ψ) stands for a convex entropy-entropy flux pair :

$$\left(\nabla \psi(\boldsymbol{w})\right)^T = \left(\nabla s(\boldsymbol{w})\right)^T \ D_{\boldsymbol{w}} \boldsymbol{f}(\boldsymbol{w})$$

Entropy inequality $\simeq$ "smoothness indicator"

Croisille J.-P., *Contribution à l'Étude Théorique et à l'Approximation par Éléments Finis du Système Hyperbolique de la Dynamique des Gaz Multidimensionnelle et Multiespèces*, PhD thesis, Université de Paris VI, 1991

We focus on general non linear hyperbolic conservation laws

$$\begin{cases} \dfrac{\partial \boldsymbol{w}}{\partial t} + \mathrm{div}(\boldsymbol{f}(\boldsymbol{w})) = 0,\ (t,x) \in \mathbb{R}^+ \times \mathbb{R}^m \\ \boldsymbol{w}(0,x) = \boldsymbol{w}_0(x),\ x \in \mathbb{R}^m \end{cases}$$

Weak solutions satisfy

$$S = \frac{\partial s(\boldsymbol{w})}{\partial t} + \mathrm{div}(\psi(\boldsymbol{w})) \begin{cases} = & 0 & \text{for smooth solution} \\ = & 0 & \text{across rarefaction} \\ < & 0 & \text{across shock} \end{cases}$$

where (s, ψ) stands for a convex entropy-entropy flux pair :

$$(\nabla \psi_i(\boldsymbol{w}))^T = (\nabla s(\boldsymbol{w}))^T \ D_{\boldsymbol{w}} \boldsymbol{f}_i(\boldsymbol{w}), \quad i = 1, \ldots, d$$

Entropy inequality $\simeq$ "smoothness indicator"

Croisille J.-P., *Contribution à l'Étude Théorique et à l'Approximation par Éléments Finis du Système Hyperbolique de la Dynamique des Gaz Multidimensionnelle et Multiespèces*, PhD thesis, Université de Paris VI, 1991

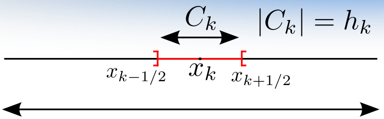

Figure: a cell C_k

Finite volume approximation :

$$\boldsymbol{w}_k^{n+1} = \boldsymbol{w}_k^n - \frac{\delta t_n}{h_k}\left(\boldsymbol{F}_{k+1/2}^n - \boldsymbol{F}_{k-1/2}^n\right)$$

with

$$\boldsymbol{w}_k^n \simeq \frac{1}{h_k}\int_{C_k} \boldsymbol{w}\left(t_n, x\right)\, dx \text{ and } \boldsymbol{F}_{k+1/2}^n \approx \frac{1}{\delta t}\int_{C_k} \boldsymbol{f}(t, w(t, x_{k+1/2}))\, dx$$

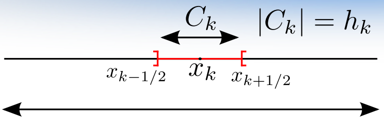

FIGURE: a cell C_k

Finite volume approximation :

$$\boldsymbol{w}_k^{n+1} = \boldsymbol{w}_k^n - \frac{\delta t_n}{h_k} \left(\boldsymbol{F}_{k+1/2}^n - \boldsymbol{F}_{k-1/2}^n \right)$$

with

$$\boldsymbol{w}_k^n \simeq \frac{1}{h_k} \int_{C_k} \boldsymbol{w}\,(t_n, x)\; dx \text{ and } \boldsymbol{F}_{k+1/2}^n \approx \frac{1}{\delta t} \int_{C_k} \boldsymbol{f}(t, w(t, x_{k+1/2}))\; dx$$

The numerical density of entropy production :

$$S_k^n = \frac{s_k^{n+1} - s_k^n}{\delta t_n} + \frac{\psi_{k+1/2}^n - \psi_{k-1/2}^n}{h_k} \lessapprox 0$$

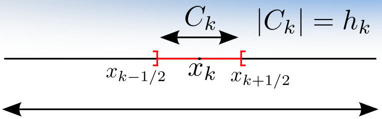

FIGURE: a cell C_k

Finite volume approximation :

$$\boldsymbol{w}_k^{n+1} = \boldsymbol{w}_k^n - \frac{\delta t_n}{h_k}\left(\sum_a \boldsymbol{F}(\boldsymbol{w}_k^n, \boldsymbol{w}_a^n; n_{k/a})\right), \quad h_k = \frac{|C_k|}{\sum_a |\partial C_{k/a}|}$$

with

$$\boldsymbol{w}_k^n \simeq \frac{1}{h_k}\int_{C_k} \boldsymbol{w}(t_n, x)\, dx, \quad \text{and } \boldsymbol{F}(\boldsymbol{w}_k^n, \boldsymbol{w}_a^n; n_{k/a}) \approx \frac{1}{\delta t}\int_{\partial C_k} \boldsymbol{f}(t, w)\cdot n_{k/a}\, ds$$

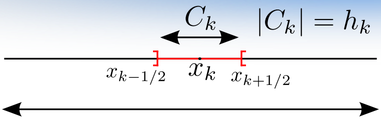

Figure: a cell C_k

Finite volume approximation :

$$\boldsymbol{w}_k^{n+1} = \boldsymbol{w}_k^n - \frac{\delta t_n}{h_k}\left(\sum_a \boldsymbol{F}(\boldsymbol{w}_k^n, \boldsymbol{w}_a^n; n_{k/a})\right), \quad h_k = \frac{|C_k|}{\sum_a |\partial C_{k/a}|}$$

with

$$\boldsymbol{w}_k^n \simeq \frac{1}{h_k}\int_{C_k} \boldsymbol{w}(t_n, x)\, dx, \quad \text{and } \boldsymbol{F}(\boldsymbol{w}_k^n, \boldsymbol{w}_a^n; n_{k/a}) \approx \frac{1}{\delta t}\int_{\partial C_k} \boldsymbol{f}(t, w)\cdot n_{k/a}\, ds$$

The numerical density of entropy production :

$$S_k^n = \frac{s_k^{n+1} - s_k^n}{\delta t_n} + \frac{\sum_a \psi(\boldsymbol{w}_k^n, \boldsymbol{w}_a^n; n_{k/a})}{h_k} \lessapprox 0$$

Mesh refinement indicator : principle & illustration

- Given $w_k^n \to$ compute w_k^{n+1}

- Given $w_k^n \rightarrow$ compute w_k^{n+1}
- Compute S_k^n : $S_k^n \neq 0 \Longrightarrow$ the cell is refined or coarsened

- Given $w_k^n \to$ compute w_k^{n+1}
- Compute S_k^n : $S_k^n \neq 0 \Longrightarrow$ the cell is refined or coarsened
- More precisely :
  - $S_k^n \leqslant \alpha_{\mathsf{min}} \overline{S} \Longrightarrow$ the cell is refined with $\overline{S} = \dfrac{1}{|\Omega|} \displaystyle\int_\Omega S_k^n$

Mesh refinement indicator : principle & illustration

- Given $w_k^n \to$ compute w_k^{n+1}
- Compute S_k^n : $S_k^n \neq 0 \Longrightarrow$ the cell is refined or coarsened
- More precisely :
  - $S_k^n \leqslant \alpha_{\mathsf{min}} \overline{S} \Longrightarrow$ the cell is refined with $\overline{S} = \dfrac{1}{|\Omega|} \displaystyle\int_\Omega S_k^n$
  - $S_k^n \geqslant \alpha_{\mathsf{max}} \overline{S} \Longrightarrow$ the cell is coarsened

- Given $w_k^n \to$ compute w_k^{n+1}
- Compute S_k^n : $S_k^n \neq 0 \Longrightarrow$ the cell is refined or coarsened
- More precisely :
  - $S_k^n \leqslant \alpha_{\text{min}} \overline{S} \Longrightarrow$ the cell is refined with $\overline{S} = \dfrac{1}{|\Omega|} \displaystyle\int_\Omega S_k^n$
  - $S_k^n \geqslant \alpha_{\text{max}} \overline{S} \Longrightarrow$ the cell is coarsened
  - Dynamic mesh refinement :
    - ⋆ Dyadic tree (1D)
    - ⋆ hierarchical numbering : basis 2

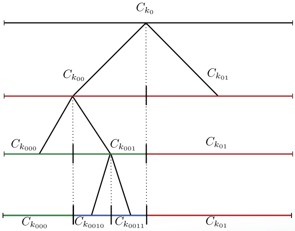

- Given $w_k^n \to$ compute w_k^{n+1}
- Compute S_k^n : $S_k^n \neq 0 \Longrightarrow$ the cell is refined or coarsened
- More precisely :
  - $S_k^n \leqslant \alpha_{\text{min}} \overline{S} \Longrightarrow$ the cell is refined with $\overline{S} = \dfrac{1}{|\Omega|} \displaystyle\int_\Omega S_k^n$
  - $S_k^n \geqslant \alpha_{\text{max}} \overline{S} \Longrightarrow$ the cell is coarsened
  - Dynamic mesh refinement :
    - ⋆ Non-structured grid : macro-cell
    - ⋆ Dyadic tree (1D), Quadtree (2D)
    - ⋆ hierarchical numbering : basis 2,4

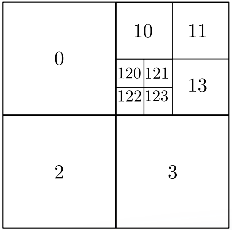

- Given $w_k^n \to$ compute w_k^{n+1}
- Compute S_k^n : $S_k^n \neq 0 \Longrightarrow$ the cell is refined or coarsened
- More precisely :
  - $S_k^n \leqslant \alpha_{\text{min}} \overline{S} \Longrightarrow$ the cell is refined with $\overline{S} = \dfrac{1}{|\Omega|} \displaystyle\int_\Omega S_k^n$
  - $S_k^n \geqslant \alpha_{\text{max}} \overline{S} \Longrightarrow$ the cell is coarsened
  - Dynamic mesh refinement :
    - Non-structured grid : macro-cell
    - Dyadic tree (1D), Quadtree (2D), Octree (3D)
    - hierarchical numbering : basis 2,4,8

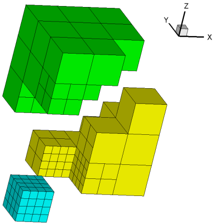

- Given $w_k^n \to$ compute w_k^{n+1}
- Compute S_k^n : $S_k^n \neq 0 \Longrightarrow$ the cell is refined or coarsened
- More precisely :
  - $S_k^n \leqslant \alpha_{\text{min}}\overline{S} \Longrightarrow$ the cell is refined with $\overline{S} = \dfrac{1}{|\Omega|}\displaystyle\int_\Omega S_k^n$
  - $S_k^n \geqslant \alpha_{\text{max}}\overline{S} \Longrightarrow$ the cell is coarsened

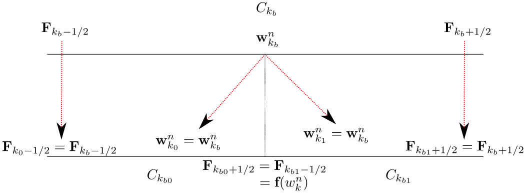

- Given $w_k^n \to$ compute w_k^{n+1}
- Compute S_k^n : $S_k^n \neq 0 \implies$ the cell is refined or coarsened
- More precisely :
  - $S_k^n \leqslant \alpha_{\text{min}} \overline{S} \implies$ the cell is refined with $\overline{S} = \dfrac{1}{|\Omega|} \displaystyle\int_\Omega S_k^n$
  - $S_k^n \geqslant \alpha_{\text{max}} \overline{S} \implies$ the cell is coarsened

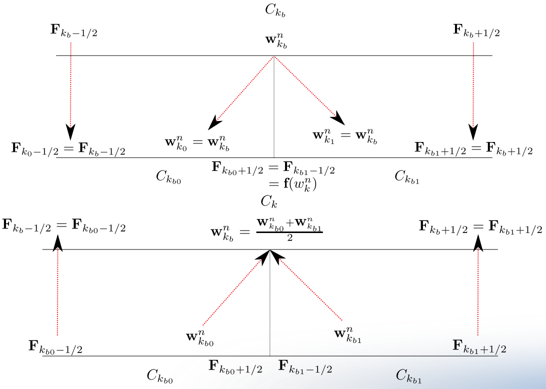

- Given $w_k^n \rightarrow$ compute w_k^{n+1}
- Compute S_k^n : $S_k^n \neq 0 \Longrightarrow$ the cell is refined or coarsened
- More precisely :
  - $S_k^n \leqslant \alpha_{\mathrm{min}}\overline{S} \Longrightarrow$ the cell is refined with $\overline{S} = \dfrac{1}{|\Omega|}\displaystyle\int_\Omega S_k^n$
  - $S_k^n \geqslant \alpha_{\mathrm{max}}\overline{S} \Longrightarrow$ the cell is coarsened
  - Simple approach but the scheme is locally non consistent [SO88, TW05]

Shu C. W., Osher S., *Efficient implementation of essentially nonoscillatory shock-capturing schemes.* J. Comput. Phys., 77(2) :439–471, 1988.

Tang H., Warnecke G., *A class of high resolution difference schemes for nonlinear Hamilton-Jacobi equations with varying time and space grids.* SIAM J. Sci. Comput., 26(4) :1415–1431, 2005.

- Given $w_k^n \to$ compute w_k^{n+1}
- Compute S_k^n : $S_k^n \neq 0 \Longrightarrow$ the cell is refined or coarsened
- More precisely :
  - $S_k^n \leqslant \alpha_{\text{min}}\overline{S} \Longrightarrow$ the cell is refined with $\overline{S} = \dfrac{1}{|\Omega|}\displaystyle\int_\Omega S_k^n$
  - $S_k^n \geqslant \alpha_{\text{max}}\overline{S} \Longrightarrow$ the cell is coarsened
  - Simple approach but the scheme is locally non consistent [SO88, TW05]
  - Limit the mesh level of adjacent cells by 2

Shu C. W., Osher S., *Efficient implementation of essentially nonoscillatory shock-capturing schemes.* J. Comput. Phys., 77(2) :439–471, 1988.

Tang H., Warnecke G., *A class of high resolution difference schemes for nonlinear Hamilton-Jacobi equations with varying time and space grids.* SIAM J. Sci. Comput., 26(4) :1415–1431, 2005.

- Given $w_k^n \to$ compute w_k^{n+1}
- Compute S_k^n : $S_k^n \neq 0 \Longrightarrow$ the cell is refined or coarsened
- More precisely :
  - $S_k^n \leqslant \alpha_{\text{min}} \overline{S} \Longrightarrow$ the cell is refined with $\overline{S} = \dfrac{1}{|\Omega|} \displaystyle\int_\Omega S_k^n$
  - $S_k^n \geqslant \alpha_{\text{max}} \overline{S} \Longrightarrow$ the cell is coarsened

  - Simple approach but the scheme is locally non consistent [SO88, TW05]
  - Limit the mesh level of adjacent cells by 2
  - A correction can be obtained (work in progress) [AE15]

Altazin T., Ersoy, M. *Analyze of the inconsistency of adaptive scheme. Preprint (in progress)*, 2015.

Shu C. W., Osher S., *Efficient implementation of essentially nonoscillatory shock-capturing schemes.* J. Comput. Phys., 77(2) :439–471, 1988.

Tang H., Warnecke G., *A class of high resolution difference schemes for nonlinear Hamilton-Jacobi equations with varying time and space grids.* SIAM J. Sci. Comput., 26(4) :1415–1431, 2005.

1. PRINCIPLE OF THE METHOD
   - Generality
   - 1d examples and local time stepping
   - Data structure : BB-AMR
2. APPLICATIONS
   - The two phase low Mach model
   - A two-dimensional dam-break problem
   - A three-dimensional dam-break problem
3. CONCLUSIONS

$$\frac{\partial \rho}{\partial t} + \frac{\partial \rho u}{\partial x} = 0$$
$$\frac{\partial \rho u}{\partial t} + \frac{\partial \left(\rho u^2 + p\right)}{\partial x} = 0$$
$$\frac{\partial \rho E}{\partial t} + \frac{\partial \left(\rho E + p\right) u}{\partial x} = 0$$
$$p = (\gamma - 1)\rho\varepsilon$$

where

$\rho(t,x)$	:	density
$u(t,x)$	:	velocity
$p(t,x)$	:	pressure
$\gamma := 1.4$	:	ratio of the specific heats
$E(\varepsilon,u)$	:	total energy
ε	:	internal specific energy
E	=	$\varepsilon + \frac{u^2}{2}$

Intel(R) Core(TM) i5-2500 CPU @ 3.30GHz

$$\begin{aligned} \frac{\partial \rho}{\partial t} + \frac{\partial \rho u}{\partial x} &= 0 \\ \frac{\partial \rho u}{\partial t} + \frac{\partial \left(\rho u^2 + p\right)}{\partial x} &= 0 \\ \frac{\partial \rho E}{\partial t} + \frac{\partial \left(\rho E + p\right) u}{\partial x} &= 0 \\ p &= (\gamma - 1)\rho\varepsilon \end{aligned}$$

where

$\rho(t,x)$	:	density
$u(t,x)$	:	velocity
$p(t,x)$	:	pressure
$\gamma := 1.4$	:	ratio of the specific heats
$E(\varepsilon,u)$	:	total energy
ε	:	internal specific energy
E	$=$	$\varepsilon + \frac{u^2}{2}$

- Conservative variables

$$\boldsymbol{w} = (\rho, \rho u, \rho E)^t$$

- entropy

$$s(\boldsymbol{w}) = -\rho \ln\left(\frac{p}{\rho^\gamma}\right) \text{ of flux } \psi(\boldsymbol{w}) = u\, s(\boldsymbol{w}) \ .$$

Intel(R) Core(TM) i5-2500 CPU @ 3.30GHz

Mesh refinement parameter $\alpha_{\max}$	:	0.01 ,
Mesh coarsening parameter $\alpha_{\min}$	:	0.001 ,
Mesh refinement parameter $\bar{S}$	:	$\dfrac{1}{\lvert\Omega\rvert}\sum_{k_b} S^n_{k_b}$
CFL	:	0.25,
Simulation time (s)	:	0.4,
Initial number of cells	:	200,
Maximum level of mesh refinement	:	$L_{\max}$.

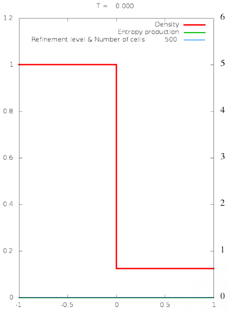

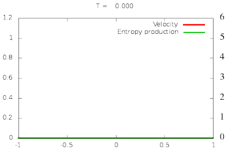

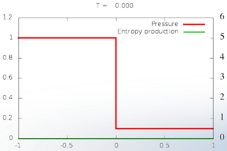

Accuracy

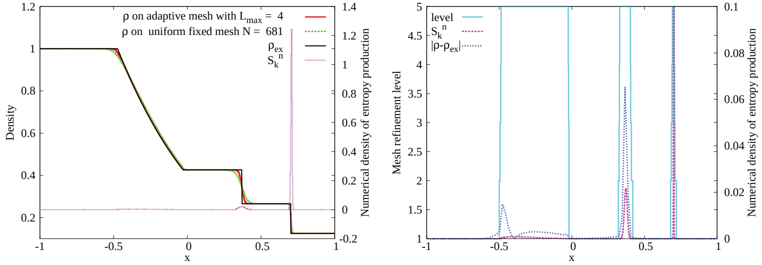

(a) Density and numerical density of entropy production.

(b) Mesh refinement level, numerical density of entropy production and local error.

Figure: Sod's shock tube problem : solution at time $t = 0.4$ s using the AB1M scheme on a dynamic grid with $L_{\max} = 5$ and the AB1 scheme on a uniform fixed grid of 681 cells.

- Explicit adaptive schemes : time consuming due to the restriction

$$\|w\|\frac{\delta t}{h} \leqslant 1, \quad h = \min_k h_k$$

- Explicit adaptive schemes : time consuming due to the restriction

$$\|w\|\frac{\delta t}{h} \leqslant 1, \quad h = \min_k h_k$$

- Local time stepping algorithm :
  - Sort cells in groups w.r.t. to their level

Muller S., Stiriba Y., *Fully adaptive multiscale schemes for conservation laws employing locally varying time stepping.* SIAM J. Sci. Comput., 30(3) :493–531, 2007.

- Explicit adaptive schemes : time consuming due to the restriction

$$\|w\|\frac{\delta t}{h} \leqslant 1, \quad h = \min_k h_k$$

- Local time stepping algorithm :
  - Sort cells in groups w.r.t. to their level
  - Update the cells following the local time stepping algorithm.

Muller S., Stiriba Y., *Fully adaptive multiscale schemes for conservation laws employing locally varying time stepping.* SIAM J. Sci. Comput., 30(3) :493–531, 2007.

- Explicit adaptive schemes : time consuming due to the restriction

$$\|w\|\frac{\delta t}{h} \leqslant 1, \quad h = \min_k h_k$$

- Local time stepping algorithm :
  - Sort cells in groups w.r.t. to their level
  - Update the cells following the local time stepping algorithm.
  - save the cpu-time keeping the accuracy.

M. Ersoy, F. Golay, L. Yushchenko. *Adaptive multi-scale scheme based on numerical entropy production for conservation laws.* CEJM, Central European Journal of Mathematics, 11(8), pp 1392-1415, 2013.

M. Ersoy, F. Golay, L. Yushchenko. Adaptive scheme based on entropy production : robustness through severe test cases for hyperbolic conservation laws. *Preprint*, https://hal.archives-ouvertes.fr/hal-00918773, 2013.

Outline

1. Principle of the method
   - Generality
   - 1d examples and local time stepping
   - Data structure : BB-AMR
2. Applications
   - The two phase low Mach model
   - A two-dimensional dam-break problem
   - A three-dimensional dam-break problem
3. Conclusions

- Main difficulty : mesh and data structure.
  For fast computation, the following are required
  - parallel treatment
  - hierarchical grids

- Main difficulty : mesh and data structure.
  Some interesting issues :
  - 2D quad-tree [ZW11],
  - 3D octree [LGF04],
  - 2D/3D anisotropic AMR [HFCC13].

Zhang, M., and W.M. Wu. 2011. *A two dimensional hydrodynamic and sediment transport model for dam break based on finite volume method with quadtree grid.* Applied Ocean Research 33 (4) : 297 – 308.

Losasso, F., F. Gibou, and R. Fedkiw. 2004. *Simulating Water and Smoke with an Octree Data Structure.* ACM Trans. Graph. 23 (3) : 457–462, 2004.

Hachem, E., S. Feghali, R. Codina, and T. Coupez. *Immersed stress method for fluid structure interaction using anisotropic mesh adaptation.* International Journal for Numerical Methods in Engineering 94 (9) : 805–825, 2013.

- Main difficulty : mesh and data structure.
- The strategy adopted :

- Main difficulty : mesh and data structure.
- The strategy adopted :
  1. 1 fixed domain= 1 fixed block=1 cpu : "failure" $\rightarrow$ synchronization depends on the finest domain

- Main difficulty : mesh and data structure.
- The strategy adopted :
  1. 1 fixed domain= 1 fixed block=1 cpu : "failure" $\rightarrow$ synchronization depends on the finest domain
  2. 1 dynamic domain= n $\times$ static blocks = 1cpu : "good compromise" $\rightarrow$ each domain has almost the same number number of cells $\rightarrow$ "better" synchronization = Block-Based Adaptive Mesh Refinement (BB-AMR)

- Main difficulty : mesh and data structure.
- The strategy adopted :
  1. 1 fixed domain= 1 fixed block=1 cpu : "failure" → synchronization depends on the finest domain
  2. 1 dynamic domain= n × static blocks = 1cpu : "good compromise" → each domain has almost the same number number of cells → "better" synchronization = Block-Based Adaptive Mesh Refinement (BB-AMR)
  3. It certainly exists better strategy . . .

How it works ?

- each domain has almost the same number of cells

How it works ?

- each domain has almost the same number of cells
- domain are defined using Cuthill-McKee numbering

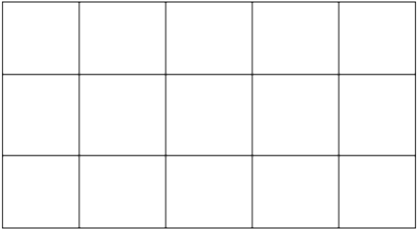

How it works ?

- each domain has almost the same number of cells
- domain are defined using Cuthill-McKee numbering

6	9			
3	5	8		
1	2	4	7	

How it works ?

- each domain has almost the same number of cells
- domain are defined using Cuthill-McKee numbering

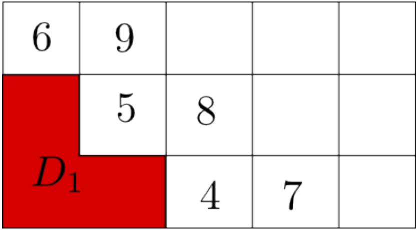

How it works ?

- each domain has almost the same number of cells
- domain are defined using Cuthill-McKee numbering

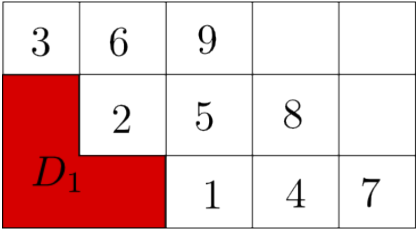

How it works ?

- each domain has almost the same number of cells
- domain are defined using Cuthill-McKee numbering

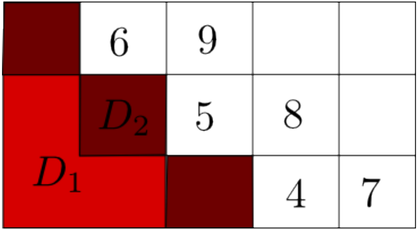

How it works ?

- each domain has almost the same number of cells
- domain are defined using Cuthill-McKee numbering

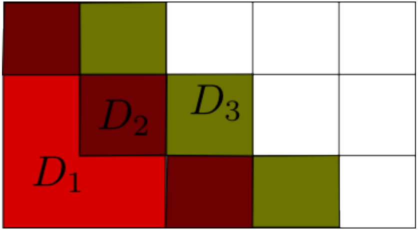

How it works ?

- each domain has almost the same number of cells
- domain are defined using Cuthill-McKee numbering

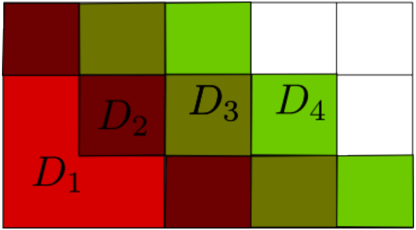

How it works ?

- each domain has almost the same number of cells
- domain are defined using Cuthill-McKee numbering

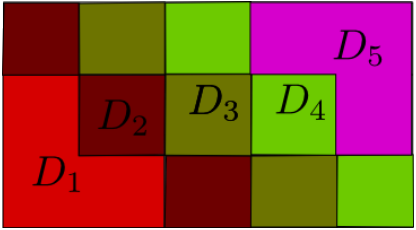

How it works ?

- each domain has almost the same number of cells
- domain are defined using Cuthill-McKee numbering
- more sophisticated numbering exists ...

How it works ?

- each domain has almost the same number of cells
- domain are defined using Cuthill-McKee numbering
- more sophisticated numbering exists . . .
- re-numbering and re-meshing being expensive
  - the mesh should be kept constant on a time interval

How it works ?

- each domain has almost the same number of cells
- domain are defined using Cuthill-McKee numbering
- more sophisticated numbering exists ...
- re-numbering and re-meshing being expensive
    - the mesh should be kept constant on a time interval
    - AMR time-step computed through the smallest block and not the smallest cell $T_{n+1} - T_n = \Delta T_{\mathrm{AMR}}$ is given by the CFL

$$\Delta T_{\mathrm{AMR}} \leqslant \beta \frac{\min_k h_{\mathrm{block_k}}}{\max_k \left\| \boldsymbol{u}_{\mathrm{block_k}} \right\|}, \; 0 < \beta \leqslant 1.$$

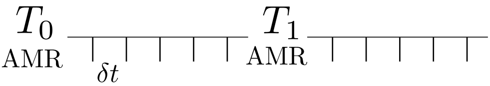

How it works ?

- each domain has almost the same number of cells
- domain are defined using Cuthill-McKee numbering
- more sophisticated numbering exists . . .
- re-numbering and re-meshing being expensive
  - the mesh should be kept constant on a time interval
  - AMR time-step computed through the smallest block and not the smallest cell
  - Gain is important and numerical stability is conserved !

Thomas Altazin, Mehmet Ersoy, Frédéric Golay, Damien Sous, and Lyudmyla Yushchenko. *Numerical entropy production for multidimensional conservation laws using Block-Based Adaptive Mesh Refinement scheme.* preprint, 2015.

- A two dimensional example of BB-AMR with 3 domains and 9 blocks.

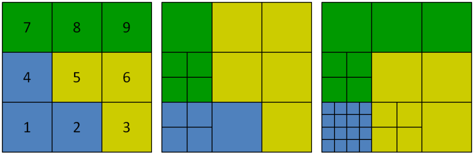

(a) AMR T_0 (b) AMR T_1 (c) AMR T_2

- A two dimensional example of BB-AMR with 3 domains and 9 blocks.

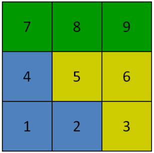

(f) AMR T_0

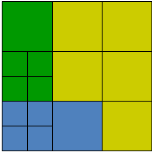

(g) AMR T_1

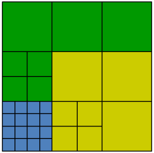

(h) AMR T_2

- A three dimensional example of BB-AMR with 3 domains and 27 blocks.

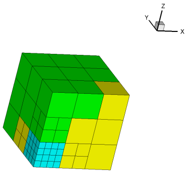

(i) Block-based mesh

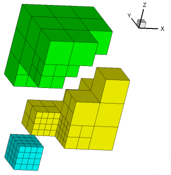

(j) Domain decomposition

OUTLINE

1. PRINCIPLE OF THE METHOD
   - Generality
   - 1d examples and local time stepping
   - Data structure : BB-AMR
2. APPLICATIONS
   - The two phase low Mach model
   - A two-dimensional dam-break problem
   - A three-dimensional dam-break problem
3. CONCLUSIONS

- Understanding of wave hydrodynamics is of primary interest for ocean and naval engineering applications :
  - dynamics of ships and floating structures,
  - stability of offshore structures,
  - coastal erosion and submersion processes, ...

- Understanding of wave hydrodynamics is of primary interest for ocean and naval engineering applications :
- It's difficult to describe accurately wave dynamics and still a fairly open research field.
  breaking or impacting waves on rigid structures = violent transformations

- Understanding of wave hydrodynamics is of primary interest for ocean and naval engineering applications :
- It's difficult to describe accurately wave dynamics and still a fairly open research field.
- involved physical processes, such as splash-ups or gas pockets entrapment, are quite complex and can hardly be characterized by field or laboratory experiments or analytical approaches : several models ! :

- Understanding of wave hydrodynamics is of primary interest for ocean and naval engineering applications :
- It's difficult to describe accurately wave dynamics and still a fairly open research field.
- involved physical processes, such as splash-ups or gas pockets entrapment, are quite complex and can hardly be characterized by field or laboratory experiments or analytical approaches : several models ! :
- Therefore, numerical simulation of breaking and impacting waves is both
  - an attractive research topic
  - a challenging task for coastal and environmental engineering

OUTLINE

1. PRINCIPLE OF THE METHOD
   - Generality
   - 1d examples and local time stepping
   - Data structure : BB-AMR

2. APPLICATIONS
   - The two phase low Mach model
   - A two-dimensional dam-break problem
   - A three-dimensional dam-break problem

3. CONCLUSIONS

- Assumptions : physics of impacting/breaking waves can be simplified
  - mainly governed by pressure forces and overturning forces
  - Mach number $< 0.3 \rightarrow$ fluid is slightly compressible

- Assumptions : physics of impacting/breaking waves can be simplified
  - mainly governed by pressure forces and overturning forces
  - Mach number $< 0.3 \rightarrow$ fluid is slightly compressible
  - small-scale friction and dissipation process are neglected

- Assumptions : physics of impacting/breaking waves can be simplified
  - mainly governed by pressure forces and overturning forces
  - Mach number $< 0.3 \to$ fluid is slightly compressible
  - small-scale friction and dissipation process are neglected
  - two-phase flow Compressible Euler equations can be considered

- Model (2D and 3D) : low mach two phase

$$\frac{\partial \rho}{\partial t} + \text{div}(\rho u) = 0$$
$$\frac{\partial \rho u}{\partial t} + \text{div}\left(\rho u^2 + pI\right) = \rho g$$
$$\frac{\partial \varphi}{\partial t} + u \cdot \nabla \varphi = 0$$

where

$\rho(t,x)$	:	density
$u(t,x)$	:	velocity
$p(t,x)$	:	pressure
φ	:	fluid's fraction

- Assumptions : physics of impacting/breaking waves can be simplified
  - mainly governed by pressure forces and overturning forces
  - Mach number $< 0.3 \to$ fluid is slightly compressible
  - small-scale friction and dissipation process are neglected
  - two-phase flow Compressible Euler equations can be considered
  - An artificial linearized pressure law is used to compute low Mach flows [C67]
- Model (2D and 3D) : low mach two phase

$$\frac{\partial \rho}{\partial t} + \text{div}(\rho u) = 0$$
$$\frac{\partial \rho u}{\partial t} + \text{div}\left(\rho u^2 + pI\right) = \rho g$$
$$\frac{\partial \varphi}{\partial t} + u \cdot \nabla \varphi = 0$$

where

$\rho(t,x)$	:	density
$u(t,x)$	:	velocity
$p(t,x)$	:	pressure
φ	:	fluid's fraction

with $p = p_0 + c_0\left(\rho - (\varphi\rho_w + (1-\varphi)\rho_a)\right)$

Chorin, A.J. . *A Numerical Method for Solving Incompressible Viscous Flow Problems.* Journal of Computational Physics 2 (1) : 12 – 26, 1967

- Assumptions
- Model (2D and 3D) : low mach two phase

$$\frac{\partial \rho}{\partial t} + \text{div}(\rho u) = 0$$
$$\frac{\partial \rho u}{\partial t} + \text{div}\left(\rho u^2 + pI\right) = \rho g$$
$$\frac{\partial \varphi}{\partial t} + u \cdot \nabla \varphi = 0$$

where

$\rho(t,x)$	:	density
$u(t,x)$	:	velocity
$p(t,x)$	:	pressure
φ	:	fluid's fraction

with $p = p_0 + c_0\left(\rho - (\varphi\rho_w + (1-\varphi)\rho_a)\right)$

- Equation of state with artificial sound speed → CFL less restrictive

- Assumptions
- Model (2D and 3D) : low mach two phase

$$\frac{\partial \rho}{\partial t} + \text{div}(\rho u) = 0$$
$$\frac{\partial \rho u}{\partial t} + \text{div}\left(\rho u^2 + pI\right) = \rho g$$
$$\frac{\partial \varphi}{\partial t} + u \cdot \nabla \varphi = 0$$

where

$\rho(t,x)$	:	density
$u(t,x)$	:	velocity
$p(t,x)$	:	pressure
φ	:	fluid's fraction

with $p = p_0 + c_0\left(\rho - (\varphi\rho_w + (1-\varphi)\rho_a)\right)$

- Equation of state with artificial sound speed → CFL less restrictive
- Explicit scheme → easy parallel implementation (MPI)

- Assumptions
- Model (2D and 3D) : low mach two phase

$$\frac{\partial \rho}{\partial t} + \text{div}(\rho u) = 0$$
$$\frac{\partial \rho u}{\partial t} + \text{div}\left(\rho u^2 + pI\right) = \rho g$$
$$\frac{\partial \varphi}{\partial t} + u \cdot \nabla \varphi = 0$$

where

$\rho(t,x)$	:	density
$u(t,x)$	:	velocity
$p(t,x)$	:	pressure
φ	:	fluid's fraction

with $p = p_0 + c_0\left(\rho - (\varphi\rho_w + (1-\varphi)\rho_a)\right)$

- Equation of state with artificial sound speed → CFL less restrictive
- Explicit scheme → easy parallel implementation (MPI)

  ✅ hyperbolic system

- Moreover,

- Assumptions
- Model (2D and 3D) : low mach two phase

$$\frac{\partial \rho}{\partial t} + \text{div}(\rho u) = 0$$
$$\frac{\partial \rho u}{\partial t} + \text{div}\left(\rho u^2 + pI\right) = \rho g$$
$$\frac{\partial \varphi}{\partial t} + u \cdot \nabla \varphi = 0$$

where

$\rho(t,x)$	:	density
$u(t,x)$	:	velocity
$p(t,x)$	:	pressure
φ	:	fluid's fraction

with $p = p_0 + c_0\left(\rho - (\varphi\rho_w + (1-\varphi)\rho_a)\right)$

- Equation of state with artificial sound speed → CFL less restrictive
- Explicit scheme → easy parallel implementation (MPI)
- Moreover,
  - ☑ hyperbolic system
  - ☑ entropy available

- Assumptions
- Model (2D and 3D) : low mach two phase

$$\frac{\partial \rho}{\partial t} + \text{div}(\rho u) = 0$$
$$\frac{\partial \rho u}{\partial t} + \text{div}\left(\rho u^2 + pI\right) = \rho g$$
$$\frac{\partial \varphi}{\partial t} + u \cdot \nabla \varphi = 0$$

where

$\rho(t,x)$	:	density
$u(t,x)$	:	velocity
$p(t,x)$	:	pressure
φ	:	fluid's fraction

with $p = p_0 + c_0\left(\rho - (\varphi\rho_w + (1-\varphi)\rho_a)\right)$

- Equation of state with artificial sound speed $\rightarrow$ CFL less restrictive
- Explicit scheme $\rightarrow$ easy parallel implementation (MPI)
- Moreover,
  - ☑ hyperbolic system
  - ☑ entropy available
  - ☑ automatic mesh refinement

- Assumptions
- Model (2D and 3D) : low mach two phase

$$\frac{\partial \rho}{\partial t} + \text{div}(\rho u) = 0$$
$$\frac{\partial \rho u}{\partial t} + \text{div}\left(\rho u^2 + pI\right) = \rho g$$
$$\frac{\partial \varphi}{\partial t} + u \cdot \nabla \varphi = 0$$

where

$\rho(t,x)$	:	density
$u(t,x)$	:	velocity
$p(t,x)$	:	pressure
φ	:	fluid's fraction

with $p = p_0 + c_0\left(\rho - (\varphi\rho_w + (1-\varphi)\rho_a)\right)$

- Equation of state with artificial sound speed → CFL less restrictive
- Explicit scheme → easy parallel implementation (MPI)
- Moreover,
  - ☑ hyperbolic system
  - ☑ entropy available
  - ☑ automatic mesh refinement
  - ☑ local time stepping

Outline

1. Principle of the method
   - Generality
   - 1d examples and local time stepping
   - Data structure : BB-AMR
2. Applications
   - The two phase low Mach model
   - A two-dimensional dam-break problem
   - A three-dimensional dam-break problem
3. Conclusions

A two-dimensional dam-break problem [KTO95]

- capture the complex structure of the air-water interface after wave impact

Koshizuka, S., H. Tamako, and Y. Oka. *A particle method for incompressible viscous flow with fluid fragmentations.* Computational Fluid Dynamics Journal, 4 (1) : 29–46, 1995.

- capture the complex structure of the air-water interface after wave impact
- Experimental configuration

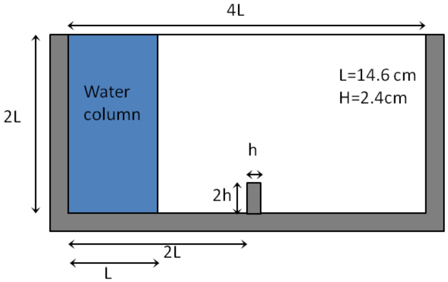

- capture the complex structure of the air-water interface after wave impact
- Numerical parameters :

Mesh refinement parameter $\alpha_{\max}$	:	0.2 ,
Mesh coarsening parameter $\alpha_{\min}$	:	0.02 ,
Number of domain	:	321,
Number of blocks	:	321,
Number of processors	:	120,
Maximum level of mesh refinement	:	$L_{\max} = 5$,
CFL	:	$CFL = 0.8$,
Simulation time	:	$T = 1.5$,
AMR time	:	$AMR = 300$.

- capture the complex structure of the air-water interface after wave impact
- Confrontation with experiments : $T = 0$

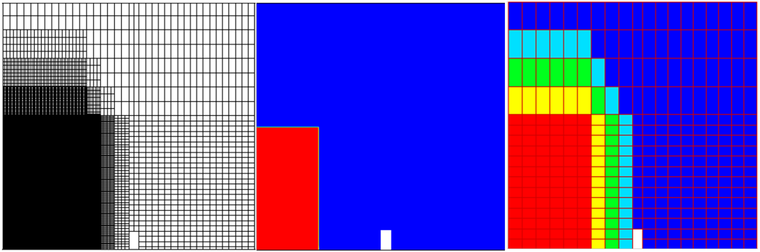

FIGURE: mesh (left), density with blue and red corresponding to air and water, respectively (center), mesh refinement level (1 to 5) per block (right)

- capture the complex structure of the air-water interface after wave impact
- Confrontation with experiments : $T = 0.2$

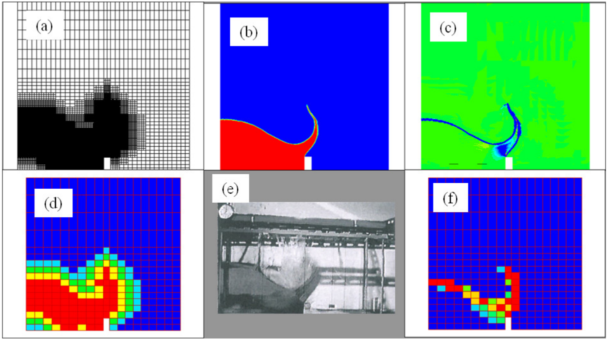

FIGURE: (a) Mesh ; (b) Density (air-blue, water-red) ; (c) Density of numerical entropy production (green-zero, blue-negative values) ; (d) Mesh refinement level per block (1 to 5) ; (e) Experiment ; (f) Mesh refinement criterion per block.

- capture the complex structure of the air-water interface after wave impact
- Confrontation with experiments : $T = 0.4$

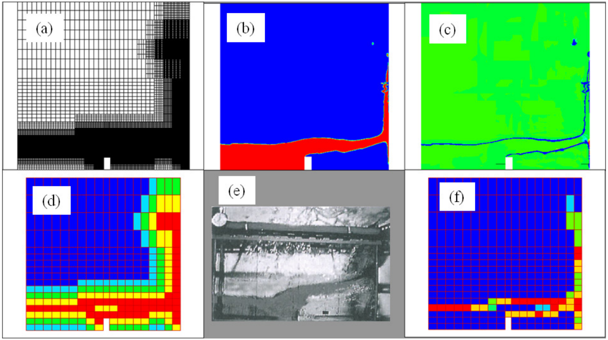

FIGURE: (a) Mesh ; (b) Density (air-blue, water-red) ; (c) Density of numerical entropy production (green-zero, blue-negative values) ; (d) Mesh refinement level per block (1 to 5) ; (e) Experiment ; (f) Mesh refinement criterion per block.

- capture the complex structure of the air-water interface after wave impact
- Remarks :
  - number of cells varies from 70 000 and 100 000
  - elapsed computing time about 5 hours
  - 1 domain = 1 block → better results with BB-AMR.

1. PRINCIPLE OF THE METHOD
   - Generality
   - 1d examples and local time stepping
   - Data structure : BB-AMR
2. APPLICATIONS
   - The two phase low Mach model
   - A two-dimensional dam-break problem
   - A three-dimensional dam-break problem
3. CONCLUSIONS

A three-dimensional dam-break problem [K05]

- capture the complex structure of the air-water interface after wave impact

Kleefsman, K.M.T., G. Fekken, A.E.P. Veldman, B. Iwanowski, and B. Buchner. *A Volume-of-Fluid based simulation method for wave impact problems.* Journal of Computational Physics 206 (1) : 363 – 393, 2005.

- capture the complex structure of the air-water interface after wave impact
- Experimental configuration

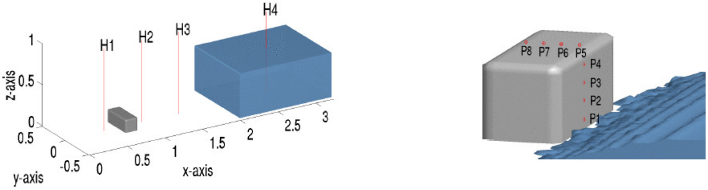

FIGURE: domain geometry and sensors points from
http://www.math.rug.nl/$\sim$veldman/comflow/dambreak.html

- capture the complex structure of the air-water interface after wave impact
- Numerical parameters :

Mesh refinement parameter $\alpha_{\max}$	:	0.2 ,
Mesh coarsening parameter $\alpha_{\min}$	:	0.02 ,
Number of domain	:	48,
Number of blocks	:	3628,
Number of processors	:	48,
Maximum level of mesh refinement	:	$L_{\max} = 4$,
CFL	:	$CFL = 0.8$,
Simulation time	:	$T = 4.8$,
AMR time	:	$AMR = 240$.

2. 48 Intel X5675 cores

- capture the complex structure of the air-water interface after wave impact
- Confrontation with experiments :

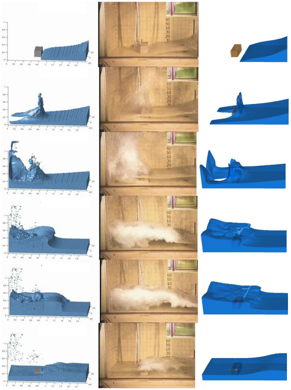

FIGURE: Free surface computed by Kleefsman (left), the experimentation (center) and our (right) at t = 0.4, 0.6, 1, 1.8, 2, 4.8s

- capture the complex structure of the air-water interface after wave impact
- Confrontation with experiments :

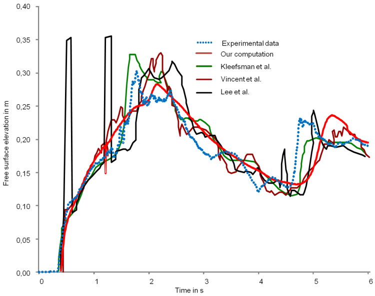

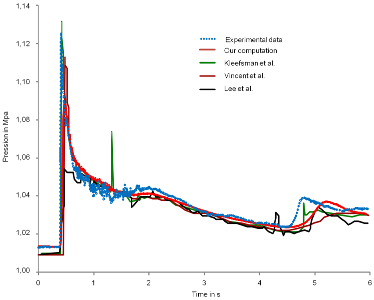

Lee, E.S., D. Violeau, R. Issa, and S. Ploix. *Application of weakly compressible and truly incompressible SPH to 3-D water collapse in waterworks.* Journal of Hydraulic Research 48 (sup1) : 50–60, 2010.

Vincent, S., G. Balmigère, J.-P. Caltagirone, and E. Meillot. *Eulerian-Lagrangian multiscale methods for solving scalar equations - Application to incompressible two-phase flows.* Journal of Computational Physics 229 (1) : 73 – 106, 2010

- capture the complex structure of the air-water interface after wave impact
- Confrontation with experiments :

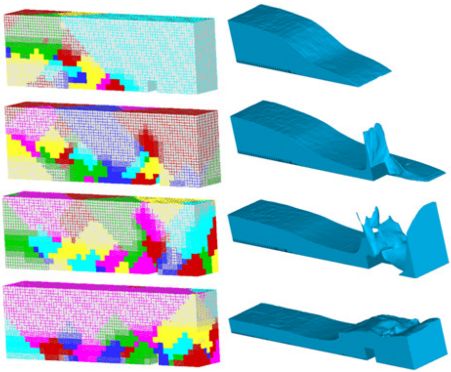

Figure: Domains due to the BB-AMR scheme (left) and air-water interface (right) at time $0.4s, 0.6s, 1.0s, 2s$.

- capture the complex structure of the air-water interface after wave impact
- Remarks :
  - number of cells varies from 800 000 cells up to about 1 500 000 cells
  - elapsed computing time about 10 hours (instead of 24h [GH07])

Golay, F., and P. Helluy. *Numerical schemes for low Mach wave breaking.* International Journal of Computational Fluid Dynamics 21(2) : 69–86, 2007.

YUSHCHENKO, L., GOLAY, F., ERSOY, M. *Production d'entropie et raffinement de maillage. Application au déferlement de vague.* 21ème Congrès Francais de Mécanique, 26 au 30 aout 2013, Bordeaux, France (FR).

Golay, F., Ersoy, M., Yushchenko, L., Sous, D. *Block-based adaptive mesh refinement scheme using numerical density of entropy production for three-dimensional two-fluid flows.* International Journal of Computational Fluid Dynamics 29.1, 67-81, 2015.

- A “block” dam break problem with a confrontation of RK2 and AB2

Thomas Altazin, Mehmet Ersoy, Frédéric Golay, Damien Sous, and Lyudmyla Yushchenko. *Numerical entropy production for multidimensional conservation laws using Block-Based Adaptive Mesh Refinement scheme.* preprint, 2015.

- A “block” dam break problem with a confrontation of RK2 and AB2
- Initial configuration

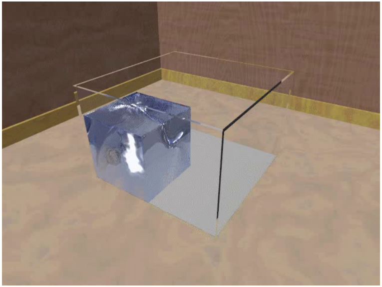

FIGURE: Unit cube $\left(\frac{1}{2} \times \frac{1}{2} \times \frac{1}{2}\right)$

- A "block" dam break problem with a confrontation of RK2 and AB2
- Numerical parameters :

Mesh refinement parameter $\alpha_{\max}$	:	0.2 ,
Mesh coarsening parameter $\alpha_{\min}$	:	0.02 ,
Number of domain	:	$1, 2, 4, 8, 32,$
Number of blocks	:	$3375,$
Number of processors	:	$40,$
Maximum level of mesh refinement	:	$L_{\max} = 4$,
Simulation time	:	$T = 2.5$,
AMR time	:	$AMR = 100$.

- A "block" dam break problem with a confrontation of RK2 and AB2
- Confrontation with experiments :

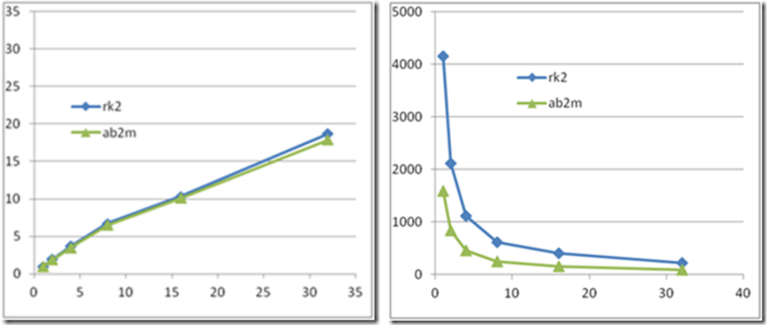

(a) Speed up vs proc number

(b) cpu time vs proc number

Figure: AB2 vs RK2

- A "block" dam break problem with a confrontation of RK2 and AB2
- Remarks :
  - number of cells varies from 172215 cells up to about 587763 cells
  - The efficiency, i.e. $\dfrac{\text{speed up}}{\text{number of processors}}$, of the computation is roughly 85% for 8 domains and 60% for 32 domains.
  - performance decrease after 20 processors $\rightarrow$ optimization is required to get more efficiency.

OUTLINE

1 PRINCIPLE OF THE METHOD
- Generality
- 1d examples and local time stepping
- Data structure : BB-AMR

2 APPLICATIONS
- The two phase low Mach model
- A two-dimensional dam-break problem
- A three-dimensional dam-break problem

3 CONCLUSIONS

- Several numerical validation on Euler equations

- Several numerical validation on Euler equations
- Several numerical validation (in progress) for shallow water equations

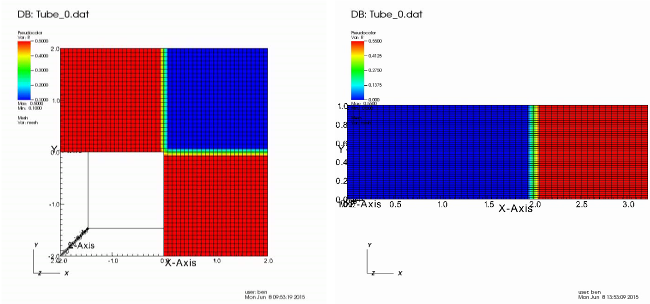

Figure: (left) L and (right) Kleefsman test case (B. Cleirec)

- Several numerical validation on Euler equations
- Several numerical validation (in progress) for shallow water equations
- local consistency error between two adjacent cells of different levels

- Several numerical validation on Euler equations
- Several numerical validation (in progress) for shallow water equations
- local consistency error between two adjacent cells of different levels
- capture accurately rarefactions and contact discontinuities

- Several numerical validation on Euler equations
- Several numerical validation (in progress) for shallow water equations
- local consistency error between two adjacent cells of different levels
- capture accurately rarefactions and contact discontinuities
- Develop a 'returning' wave model (as an intermediate one between the two-phase flow model and the shallow water equations)

Thank you

for your

attention